Cleavage fracture of a crystal: a model which includes structural relaxations

P. Lazar

Institute of General Physics, Vienna University of Technology, Getreidemarkt 9, A-1000 Vienna, Austria

R. Podloucky

Department for Physical Chemistry, University of Vienna, Sensengasse 8, A-1090, Vienna, Austria

(Dated: May 28, 2008)

Based on density functional theory calculations we present a model of cleavage under loading mode I, in which the atomic layers are allowed to relax after the crack was initiated. Based on the concept of a critical opening we derive an analytic formulation describing relaxed cleavage. The general applicability of the model is demonstrated by applications for materials with different bonding properties, such as metals, intermetallic compounds, SiC and Si. We show that the values of the critical opening are very similar to the localisation length for ideal brittle cleavage as introduced recently [Lazar et al. Appl. Phys. Lett **87**, 261910 (2005)], manifesting that at the atomic scale the elastic energy during cleavage can be described as a local property. Based on our findings, an approximate formula for the critical stress in relaxed cleavage was obtained.

I.   INTRODUCTION

A classical theory of ideal brittle fracture is based on Griffith's thermodynamic balance, which describes the stability of a crack in a homogeneous medium as a reversible thermodynamic system.[1] An existing crack of given size will grow, if the elastic energy release rate – the *elastic* energy being released during crack growth– equals the *cleavage* energy which is required for the formation of new fracture surfaces. Accordingly, only planes with low cleavage energy are favorable cleavage planes. In Griffith's model elastic and cleavage properties are interlinked. Following this direction, we achieved a formulation for the critical cleavage stress of ideal brittle cleavage, which involved the concept of localized elastic energy.[2] In the present paper we study the influence of structural relaxation during crack formation on cleavage properties. We design a simple model for crack formation in which the material is cleaved between single-crystalline planes. The energetics of the cleavage will be derived from *ab initio* density functional theory (DFT) calculations, which provide a reliable data base. Although the presented modelling of crack formation is very simplistic as compared to a realistic crack formation process we believe that useful new insights into critical materials properties can be gained from our results.

Ideal brittle cleavage is modelled by a geometrically rigid separation x of two blocks of a material without any relaxation of the atomic structure within the blocks (Fig.1, panel b). (It should be noted, that further on the subscript b denotes quantities related to ideal brittle cleavage). For such a process the so-called universal binding energy relation (UBER[3], see appendix) may be applied, which describes the decohesion energy $E_b(x)$ as a function of the separation x by introducing the cleavage energy G_b and the length parameter l_b as materials parameters, which also depend on the direction of cleavage. For large values of x the decohesion energy approaches G_b, and at $x = l_b$ the maximum of the stress σ_b –the critical stress (see appendix)– is reached: a crack is then supposed to grow when the external stress concentrated at a crack tip exceeds σ_b. UBER works well for almost all classes of materials and directions.[4],[5]

If, however, during the cleavage process structural relaxation is allowed (Fig.1, panel c), the law for the decohesion energy $E_r(x)$ must be different from that for $E_b(x)$. (It should be noted, that further on the subscript r denotes quantities related to the relaxed cleavage process). In the present work we now study the relaxed cleavage process by allowing in the DFT calculations for the relaxation of atomic layers near to the cleavage surfaces. We present results for materials with different types of bonding, including metals, intermetallic compounds, the refractory compound SiC and covalently bonded Si. In particular, we investigate the concept of localized elastic energy, as introduced recently.[2]

Section III A presents an analytical formulation of a simple model for relaxed cleavage, which introduces the relaxed cleavage energy G_r and the critical opening l_r, similar to the parameter l_b of ideal brittle cleavage; i.e. for $x > l_r$ the crack opens. The applicability of this model is checked by fitting to it DFT data of a variety of materials. In Sec. III B, we discuss that for all inspected materials and cleavage directions the values for l_r are strikingly similar to the length L_b, which was introduced as localization length for the elastic energy in our previous study on ideal brittle cleavage.[2] Finally, in Sec. III C results and quantities for ideal brittle and relaxed cleavage are compared.

II.   COMPUTATIONAL ASPECTS

For the *ab initio* DFT calculations we applied the Vienna Ab initio Simulation Package (VASP) which uses the projector augmented wave technique for the construc-

tion of the pseudopotentials.[6,7] The exchange-correlation functional was described within the generalized gradient approximation according to the parametrization of Perdew and Wang.[8] Convergence of the total energies with respect to basis size and number of **k** points for the Brillouin zone integration was carefully checked. Atomic forces were relaxed within a conjugate gradient algorithm whenever structural relaxations were required. The cleavage of a single crystal was modelled by repeated slabs of atomic layers with three-dimensional translational symmetry, which is the standard scheme for modelling surfaces by DFT approaches. Convergence of cleavage energies as a function of slab thickness and vacuum spacing was tested. The elastic constants, which are needed for the calculation of the uniaxial rigid elastic modulus, are also derived from VASP calculations,[9,10] ensuring a precision which is comparable with the cleavage results.

III. RESULTS AND DISCUSSION

A. Cleavage and structural relaxations

In the relaxed cleavage model the initial preopening x of the crack is introduced by separating two blocks of a crystalline solid (panel b of Fig. 1) as was also done for modelling ideal brittle cleavage. Now, for relaxed cleavage the atomic positions are allowed to relax after the crack opening by keeping fixed the cleavage plane area A. Structural relaxation concerns the interlayer and in-plane spacings, more complicated reconstructions of the cleavage surfaces could be taken into account but are considered to be negligible. We assume, that for openings x smaller than a critical length the crack will be healed up by elastic relaxations (panel c of Fig. 1). If, however, the critical length is exceeded the bonds between the cleavage surfaces break, the crack remains and structural relaxations only occur inside the blocks close to the surface (panel d of Fig. 1).

Following the spirit of UBER we introduce a critical opening $x = l_r$, at which the material should crack abruptly. The critical length l_r is defined as the opening, at which the elastic energy $E_r(x)$ equals the cleavage energy G_r. By definition, the opening l_r is now a local quantity independent of any macroscopic dimensions of the material. The energy $E_r(l_r) = G_r$ defines the range of openings $x < l_r$ for which crack healing by a linear elastic response occurs (as sketched in panel c of Fig. 1). Then, an obvious relation for the decohesion energy of relaxed cleavage for $x < l_r$ is achieved by

$$E_r(x) = \frac{G_r}{l_r^2} x^2 \ . \tag{1}$$

For crack sizes $x > l_r$ the energy is assumed to be constant and equal to G_r. This is of course an idealized model, because for a real material the decohesion energy
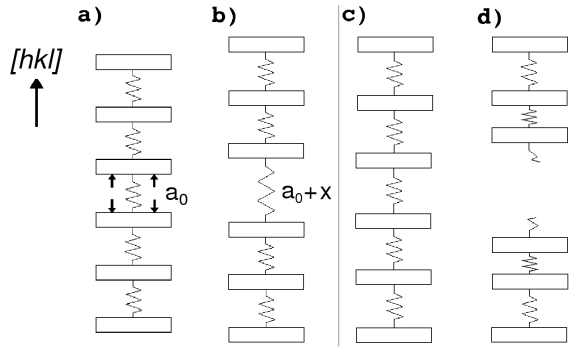

FIG. 1: Sketch of cleavage under loading mode I in direction $[hkl]$. A solid (sketched in panel a as a stacking of layers connected by spring-like bonds with a bulk layer distance a_0) undergoes ideal brittle cleavage as sketched in panel b: an opening of size x cleaves the material into two rigid blocks without relaxation of the atomic layers within the blocks. For the relaxed cleavage the material now relaxes in an elastic manner (panel c) up to a critical crack size above which it breaks into two blocks with relaxed surfaces (panel d). In all the processes, the lateral extension of the layers (i.e. the area A) remains fixed.

will deviate from the ideal elastic behavior at least close to the critical crack size, as can be seen in Fig. 2 in which the analytic model is compared to DFT results for NiAl. Nevertheless, studying many different materials and directions it turned out that the simple quadratic law is a rather reasonable approximation for relaxed cleavage, as also observed by Hayes et al.[11] studying only three cases, namely cleavage of Al in [111] direction, [0001] cleavage of Al_2O_3, and [100] cleavage of Si. In our case we arrived at the same conclusion, but now our findings are explicitly described by Eq. 1. The critical stress σ_r is defined by the first derivative,

$$\sigma_r = \left(\frac{\mathrm{d}E}{\mathrm{d}x}\right)_{x=l_r} = \frac{2G_r}{l_r} \ . \tag{2}$$

Recently, relying on a universal cohesive relation as introduced by Nguyen and Ortiz[12] a model for relaxed cleavage was suggested by Jarvis et al.[13] This model, however, depends on the *macroscopic* dimension of the material, because it involves the total number of layers for a given direction $[hkl]$. Following this concept, critical stresses for relaxed cleavage were derived, which were very small, only a fraction of the corresponding stresses for ideal brittle cleavage, which seems to be rather unphysical. In our case, which is based on intrinsic cleavage properties independent of macroscopical dimensions, we obtain stresses for relaxed cleavage which are significantly larger than for ideal brittle cleavage, as discussed in Sec. III C.

For all materials investigated in our work, the relaxed cleavage energy model fits well (for example, see Fig. 2) to the DFT data. The deviations from the simple analytic
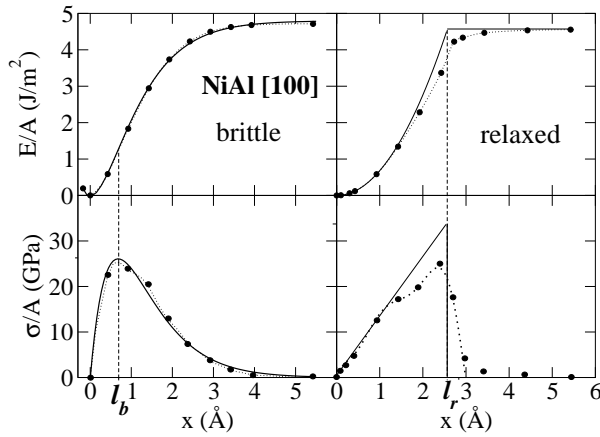
FIG. 2: Ideal brittle and relaxed cleavage in [100] direction for NiAl: decohesion energy E/A and critical stress per surface area σ/A vs. crack opening x. Full lines: analytic model of Eq.1; symbols: DFT results.

TABLE I: Model parameters for relaxed cleavage for selected materials and cleavage directions $[hkl]$: cleavage energy G_r/A (J/m^2) per surface area A. The healing length l_h is the length up to which a crack is healed up by elastic relaxations (see Fig. 3 and text), whereas l_r represents the critical length of the analytic model according to Eq. 1. At $x = l_r$ the stress for the relaxed cleavage according to Eq.2 reaches its maximum value σ_r/A (GPa). All lengths are given in units of Å .

	struct.	$[hkl]$	G_r/A	l_h	l_r	σ_r/A
Al	fcc	100	1.8	1.9	2.2	16
		110	1.9	2.2	2.4	16
		111	1.6	2.3	2.4	13
W	bcc	100	7.8	2.5	2.8	62
		110	6.4	2.1	2.1	61
NiAl	B2	100	4.6	2.5	2.5	37
		110	3.1	2.1	2.5	30
		111	3.9	2.2	2.1	35
TiAl	L1$_0$	100	3.2	2.2	2.6	25
		110	3.9	2.2	2.3	34
		001	4.2	2.6	2.7	31
Ni$_3$Al	L1$_2$	100	4.2	2.2	2.4	35
		111	3.6	2.2	2.3	31
Al$_3$Sc	L1$_2$	100	2.6	2.8	2.7	19
		110	2.9	2.9	2.6	22
		111	2.3	2.7	2.7	17
SiC	B3	111	3.8	2.1	2.2	35
Si	A4	111	2.9	1.9	1.9	30

model are significant only close to the critical opening of $x \approx l_r$. The differences between the analytic model and the DFT data are more pronounced for the stress, because it is the first derivative of the decohesion energy (see Fig 2). In Tab. I we compare the ideal critical opening l_r to the separation l_h, the healing length: for openings $x < l_h$ the crack will heal up by elastic relaxation as a result of the DFT calculations. The procedure for actiually determining l_h is illustrated in Fig. 3 showing the decohesion energies per unit area for tungsten in

two directions. There, one observes three different regions for E/A : 1) the curve is continous for $0 < x < l_h$, 2) for $l_h < x < l_f$ the curve is interrupted, and 3) for $x > l_f$ the decohesion energy again is continous, and finally approaching the cleavage energy G_r/A. For all the other studied metallic systems the splitting of E/A into the described three different regions is rather similar. The interval of crack openings $l_h < x < l_f$ indicates a region of instability: the atoms in the surface layers of the separated blocks experience forces of rather equal strength from atoms of both blocks, and consequently the procedure for relaxing the geometry by minimizing the forces does not converge well. Therefore, no sufficiently accurate decohesion energies can be derived, and the continous curve is interrupted. For values $x > l_f$ the surface layers are now attracted to their corresponding blocks and again stable relaxed atomic configurations are achieved. Finally, for sufficiently large separations (i.e. the interaction between the blocks vanishes) systems with free surfaces are described within a repeated slab scheme, which is the standard model for DFT calculations of surfaces. The instability range may be interpreted as some kind of energy barrier for breaking the material as expressed by the difference $\Delta = (E(l_f) - E(l_h))/A$, which can be quite sizeable (see Fig. 3), depending on the size of the instability range and the steepness of the function $E(x)/A$.

For Si and SiC (see Fig.4) the instability range and consequently the barrier Δ is very small, which indicates that the bonds break abruptly due to intrinsic brittleness.

Griffith's condition of thermodynamic reversibility implies that crack healing should occur for $x < l_r$. However, crack healing has very rarely been observed by experiment.[14] According to Tab. I the actual healing length l_h is smaller than the model length l_r, which would be the critical length up to which a material responds in an ideal elastic way until it abruptly breaks. For real materials, anharmonic deviations from the quadratic law will occur before the bonds actually break, and consequently the breaking of the material will happen for crack openings smaller than l_r.

The parameters for the selected materials as derived from the DFT application are summarized in Table I. For the ideal relaxed cleavage all the lengths l_r are much larger than the critical length l_b for ideal brittle cleavage (see Ref. 2). This is obvious because for relaxed cleavage the atomic structure is now allowed to relax after crack initialization, and therefore it needs larger crack sizes for finally breaking the material apart. In other words, the quadratic expression for the decohesion energy for relaxed cleavage cuts the relaxed surface energy G_r at values of l_r which are larger than the lengths l_b at which the UBER for ideal brittle cleavage has its inflection point. also the critical stress σ_r is significantly larger (by 10% up to 50%) than its counterpart σ_b for ideal brittle cleavage, as is discussed in more detail in Sec. III C.

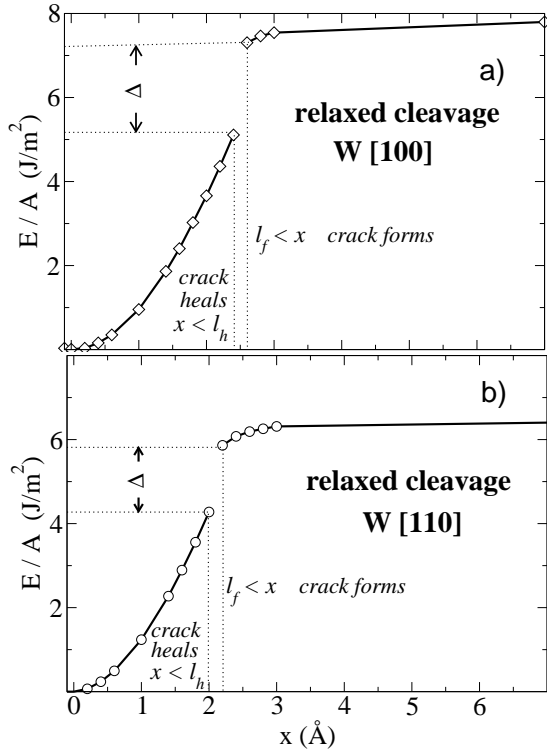The cleavage energies G_r must be smaller than their

FIG. 3: DFT results for the decohesion energy per surface area $E(x)/A$ vs. cleavage opening x for W as cleaved in the [100] (panel a) and [110] (panel b) directions. Vertical lines indicate the healing lengths l_h, up to which the crack is healed up by elastic relaxation, as well as the crack formation lengths l_f, for which the crack forms. The range Δ indicates the region of instability, as described in the text.

counterparts G_b because of the gain in relaxation energy which reduces the loss of bonding energy due to cleaving the material. In the present work we only accounted for layerwise geometrical relaxation and surface rumpling. Considering surface reconstructions -which might further lower the values of G_r- could result in very complicated atomic structures. In general, for metallic surfaces the reduction of the cleavage energy due to more complex relaxations is small; the effect of reconstructions would be more pronounced for solids with strong covalent bonds (e.g. Si[15]). Nevertheless, the general aspect of our model would remain unchanged, only the critical values l_r and σ_r would be reduced.

Tungsten is a representative example of a bcc transition metals. It is brittle at low temperatures and the bonding is strong, which in our case is reflected by the very large values for G/A and σ/A (see Tables I and II). According to the DFT results for relaxed cleavage in Fig. 3, assuming Griffith's model tungsten would preferably cleave in [110] direction, because then the cleavage energy is lowest. On the other hand, the critical stress is almost equal to that for [100] cleavage. These findings indicate similar cleavage fracture properties for both directions. From fracture experiments it was observed that W

primarily cleaves between [100] planes, but occasionally also [110] cleavage is preferred,[16]. In more recent experiments, [100] and [121] cleavage planes appeared, whereas [110] cleavage showed resistance against crack propagation.[17] A full understanding of the cleavage properties of tungsten will, however, go beyond Griffith's model because also lattice trapping effects depending on the crack front direction seem to play a significant rôle.[18]

The compounds Al_3Sc and NiAl are intermetallics, for which the bonding may be characterized as some mixture of metallic and covalent bonds. At room temperature, they are known to fail by brittle fracture. Analyzing our results, Al_3Sc has the by far lowest critical stresses and cleavage energies which reflects the rather weak bonding in comparison to NiAl, for which the bonding is of stronger, more d-like character. According to experiment polycrystalline Al_3Sc undergoes [110] transgranular cleavage at low temperatures.[19] Because its cleavage properties are rather isotropic, the preferred cleavage direction is most probably dictated by an interplay of tensile and shear stresses, and not by the lowest cleavage energy only. For NiAl, fracture experiments indicated [110] cleavage habit planes (sometimes also the higher-index [511] cleavage planes occur)[20–22]. The preference for [110] cleavage can be deduced from our results, because G/A and σ/A are lowest for the [110] direction. As a side remark, in our DFT calculations no local magnetic moment appeared during cleavage of NiAl although we allowed for spin polarization.

The intermetallic compound Ni_3Al crystallizes in the same structure as Al_3Sc, but Ni_3Al is highly ductile[23] and its alloys have the tendency to undergo brittle intergranular fracture. According to Tab. I the cleavage properties of Ni_3Al are markedly stronger than those of Al_3Sc (G/A as well as σ/A are twice as large), which may explain the quite differt fracture properties. For Ni_3Al the larger values of G/A prohibit brittle cleavage in favor of dislocation emission (see, for instance, Refs. 24,25 and references therein) or grain-boundary fracture. Furthermore, Ni_3Al shows also an interesting anisotropy of mechanical properties. The cleavage energy is by 15% larger for the [100] direction than for [111], whereas the uniaxial elastic modulus C for the [111] direction is by 50% larger than for [100]. This results demonstrate that estimates of fracture properties, which are solely based on the elastic properties, are unreliable.

Discussing relaxed [111] cleavage of Al, we obtained a value of $\sigma_r/A = 15$ GPa, which is only slightly larger than the the value for ideal brittle cleavage of $\sigma_b = 11$ GPa. Clearly, the effect of relaxation is very small, because the screening of perturbations such as the creation of a surface is strong due to the free-electron like electronic structure of Al. In Ref. 11 a layer dependent model for relaxed cleavage was applied. By that, an extremely small value for the critical stress of $\overline{\sigma}_r = 0.16$ GPa is derived for a length of 10 μm of [111] stacked Al. The comparison with our value is not possible, because the critical stress scales according to $\overline{\sigma}_r \propto 1/\sqrt{N}$ (with N
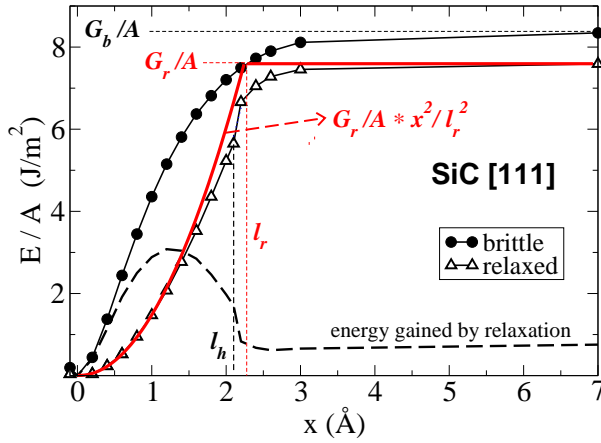
FIG. 4: (Color online) DFT derived decohesion energy per surface area $E(x)/A$ vs. crack openings x for ideal brittle (index b) and relaxed (index r) cleavage for SiC cleaved between widely spaced [111] planes of the diamond-like structure. The figure illustrates the ideal model parameter l_r and the crack healing length l_h, i.e. for $x < l_h$ the crack is healed up by elastic relaxation. The crack formation length l_f (see Fig. 3) is not drawn, because it nearly cioncides with l_h. The energy gained by structural relaxation after crack opening is obtained by substracting the decohesion energies of the relaxed case from the unrelaxed (i.e. ideal brittle cleavage) case. Furthermore, the analytical model for $E_r(x)/A$ according to Eq. 1 is also sketched. This curve is obtained by fitting its quadratic form to the DFT data for small x, at which the DFT energy is also of quadratic shape according to linear elasticity theory.

being the number of layers of the macroscopic solid) in model of Hayes *et. al.*[11]. Our model and our data for relaxed as well as brittle cleavage are independent of any macroscopic dimension of the slabs, as long as the actual slab of material is sufficiently thick which is the case. On the other, for brittle cleavage the UBER parameters of our calculation agrees perfectly with the data of Ref. 11.

The refractory compound SiC and covalently bonded Si are examples of intrinsically brittle materials, which are cleaved easiest between the widely spaced [111] planes of the diamond structure. For Si, experiments at low temperatures show brittle fracture at a load consistent with Griffith's criterion.[26] The mechanical properties are particularly interesting in this context and attracted a great deal of attention (see Refs.[26–30] and references therein). Dynamic fracture of Si was addressed in a multiscale atomistic simulation.[28] Interestingly, two length scales which emerged from the simulation -bond-breaking and elastic relaxation length scales- correspond very well to the critical lenghts l_b and relaxed cleavage l_r of our models. Obviously, atomic-level aspects of decohesion during brittle fracture are well described by a simple uniaxial cleavage model, like ours. However, a quantitative comparison of the results is difficult, because the lengths derived from the atomistic simulation of Ref. 28 depend strongly on the applied empirical potential. Our cleavage model, on the other hand, offers the advantage that it can be studied by an *ab initio* parameter-free DFT approach.

B. Localization of elastic energy in the cleavage process

Recently, the concept of localization of elastic energy has been introduced for ideal brittle cleavage[2]. The motivation was to correlate elastic and cleavage properties avoiding a non-local treatment of the elastic energy which leads to inconvenient models and rather unphysical results[11]. For the reader's convenience we elaborate our concept in more detail in the appendix. Historically, the idea of a localized elastic energy was introduced by Orowan[31] and Gilman[32], who related the elastic energy in the stressed specimen to the surface energy of the fractured faces. These authors made the ad-hoc assumption that localization occurs in a volume spanned by the surface area A and the bulk interlayer spacing a_0 along a given direction $[hkl]$. However, the results obtained by the Orowan-Gilman model turned out to be not useful. Based on DFT results for a variety of materials with different bondings we arrived at the conclusion that a_0 should be replaced by a new materials parameter, the localization length L_b for the elastic energy. It was found, that for nearly all materials and directions studied the values of L_b are in the range of 2 to 3 Å with an average value of about 2.4 Å.[2]

According to Eq. A3 all elastic energy localized in the volume AL_b is transformed into cleavage energy for ideal brittle cleavage. The area A is fixed by the bulk lattice and direction $[hkl]$. The only free parameter is L_b which is derived from fitting to cleavage properties. The length L_b might be considered as a critical length for a perturbation beyond which the crystal does not respond anymore in an elastic manner. This is exactly the case for the model for relaxed cleavage, as described by Eq.1: when cleaved by an opening x the decohesion energy is assumed to be quadratic in x up to a critical length l_r beyond which all elastic energy is converted into the cleavage energy G_r. As a consequence one therefore would expect that both critical lengths L_b and l_r are equal. Indeed, by inspection of Table II it can be observed that the agreement between the two lenghts is good or even perfect, having in mind that L_b and l_r are derived independently in totally different ways. Differences occur for two reasons: 1) fitting the quadratic part of the decohesion energy for small x may lead to errors of l_r of ± 0.1 Å; 2) for some cases at energies well below G_r the DFT data deviate significantly from the simple quadratic law, i.e. anharmonic effects become sizeable. Such cases will be discussed in the following.

Table II shows that the parameters l_r and L coincide for metals such as Al and W which are very different concerning the strength of their bonding. One also finds excellent agreement between both lengths for covalently bonded Si and SiC, the intermetallic compounds Al_3Sc

TABLE II: Calculated parameters for ideal brittle cleavage (index b) and relaxed cleavage (index r) for selected materials and cleavage directions $[hkl]$: uniaxial elastic modulus C (GPa), brittle cleavage energy G_b/A (J/m^2) per surface area A, critical length l_b, interlayer bulk distance a_0, localisation length for brittle cleavage L_b and critical stress σ_b (GPa). All lengths are given in units of Å .

	$[hkl]$	C	G_b/A	l_b	a_0	L_b	σ_b/A
Al	100	118	1.8	0.57	2.03	2.2	12
	110	127	2.1	0.64	1.43	2.5	12
	111	129	1.6	0.54	2.34	2.4	11
W	100	540	8.4	0.66	1.59	2.8	47
	110	516	6.5	0.55	2.24	2.4	44
NiAl	100	203	4.8	0.69	1.45	2.0	26
	110	284	3.2	0.54	2.05	2.5	22
	111	311	4.1	0.58	0.84	2.7	26
TiAl	100	190	3.3	0.58	2.00	2.0	21
	110	240	4.1	0.69	1.41	2.1	22
	001	185	4.4	0.70	2.03	2.1	23
Ni$_3$Al	100	225	4.3	0.66	1.78	2.3	24
	111	331	3.7	0.52	2.06	2.4	27
Al$_3$Sc	100	189	2.7	0.61	2.05	2.6	16
	110	182	2.9	0.65	1.45	2.7	16
	111	180	2.6	0.61	2.37	2.6	16
SiC	111	508	4.2	0.58	1.89	2.1	27
Si	111	189	3.1	0.54	2.36	1.8	21

FIG. 5: Critical stresses σ/A for relaxed cleavage and brittle cleavage versus the respective cleavage energies G/A. Full-line: linear least-square fit to the DFT data of relaxed cleavage (crosses); dashed-line: linear least-square fit to DFT data for brittle cleavage (squares).

were able to describe the localization of the elastic energy and to quantify the corresponding volume in terms of the lengths l_r and L_b.

C. Comparison of brittle and relaxed cleavage

Fig. 5 shows the DFT results for the critical stresses σ/A vs. cleavage energy G/A for both, relaxed and brittle cleavage, illustrating that there is some relation between stress and energy. However, estimating the critical stress directly from the cleavage energy might lead to errors of up to 20%, for relaxed as well as for ideal brittle cleavage. Therefore, assuming a direct relation between cleavage stress and cleavage energy –as was done in the pioneering work of Griffith[34] for brittle cleavage– is quantitatively not very useful.

As argued in Ref. 2 an average value of $L_b \approx 2.4$ Å may be assumed for estimating the stress within an accuracy of about $\pm 10\%$. Setting l_r equal to L_b according to the dicussion in Sec. III B, the relation $\sigma_r[\mathrm{GPa}] \approx 8.3\,G_r[\mathrm{J/m}^2]$ between the critical stress σ_r and the cleavage energy G_r is derived. Fitting the DFT data –as shown in Fig. 5– yields a prefactor of 8.5 being rather close to the estimated value of 8.3. In Fig. 5 also the results for the brittle cleavage properties are shown. By a linear fit to the DFT data we obtain the relation $\sigma_b[\mathrm{GPa}] \approx 5.6\,G_b[\mathrm{J/m}^2]$. From both relations for the critical stresses we gain the relation

$$\sigma_r \approx 1.5\sigma_b \qquad (3)$$

between the relaxed and ideal brittle cleavage stress. That means, if structural relaxation –according to our modelling– occurs during the cleavage process the critical stress is about 50% larger than for ideal brittle cleavage. (It should, however, be noted that the relation in Eq. 3

and Ni$_3$Al, in spite of the fact that for Al$_3$Sc both lengths are rather large. Exceptions occur for cleaving NiAl in [100] and [111] directions. According to Fig. 2, for the [100] direction the energy for relaxed cleavage shows a pronounced deviation from the ideal elastic behavior and a large instability region Δ. Concerning [111] cleavage, the layers stacked in this direction are very closely spaced with a value of $a_0 = 0.84$ Å and the rather large value of $L_b = 2.7$ is combined with sizeable anharmonicity effects. The second exception concerns TiAl with the tetragonal $L1_0$ structure, and occurs due to its very strong anharmonicity and anisotropy:[33] the third order elastic constant $c_{111} = -67$ GPa is exceptionally small whereas $c_{333} - 6076$ GPa is exceptionally large when compared to common metals. The unusal nonlinear elastic properties of TiAl lead to effects such as a negative volume thermal expansion down to zero Kelvin.[33]

The striking similarity of both parameters L_b and L_r implies that the concept of localization of the elastic energy in cleavage fracture is meaningful. In the process of relaxed cleavage as described above the energy of broken bonds is being converted into the elastic energy until a stable crack is opened. In a true fracture process, the elastic energy of the stressed part of the material must provide the energy for the newly cleaved fracture surfaces. Therefore, during the fracture process a large portion of the elastic energy must be present in a small volume near the crack crack. In other words, at the moment of fracture the elastic energy must localize in the vicinity of the atoms adjacent to the fracture surface. With our concept as presented in Ref. 2 and by Eq. 1 we
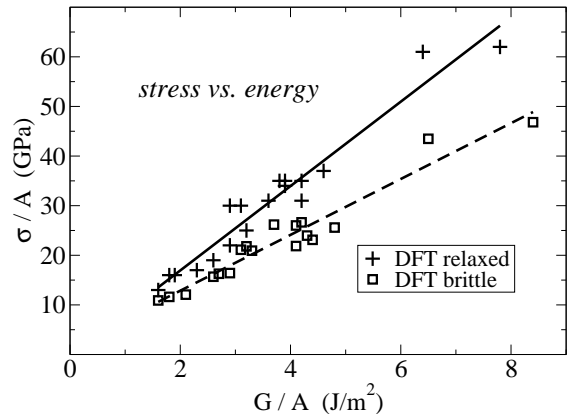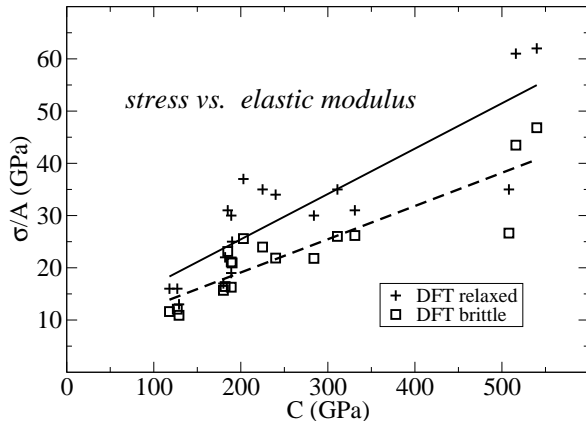
FIG. 6: Critical stresses σ/A for relaxed cleavage and brittle cleavage versus the uniaxial modulus C. Full-line: linear least-square fit to the DFT data of relaxed cleavage (crosses); dashed-line: linear least-square fit to DFT data for brittle cleavage (squares).

is a rather crude approximation, because large errors of about 30% may occur). The difference between the two stresses cannot come from the cleavage energies, because the relaxed cleavage energy G_r must be smaller than G_b: by averaging the DFT data we arrive at the averaged estimation $G_b \approx 1.06 G_r$. A plausible argument seems to be, that part of the energy, which has to be invested for the preopening of the crack, is regained by the elastic healing process and therefore the material breaks at much larger critical openings than in the ideal brittle case, i.e. $l_r \gg l_b$ (according to the Tables I, II). The actual explanation is, however, not so simple, because of the ratio

$$\sigma_r/\sigma_b = 2\mathrm{e}\frac{l_b G_r}{l_r G_b} \qquad (4)$$

which we obtained by considering Eqs. 2 and A2. Setting equal $l_r = L_b$, as argued above, and using the approximate relation between G_r and G_b one can estimate $\sigma_r/\sigma_b = 5.13 l_b/L_b$, and by assuming $L_b \approx 2.4$ Å and $l_b \approx 0.7$ Å (both are reasonable average values) we derive the factor 1.5, as it appears in Eq. 3. By making use of Eq. A4, which relates the ideal brittle cleavage stress to the uniaxial rigid modulus C we find a further relation, $\sigma_r/\sigma_b \approx 11\sqrt{G_b/AC}$: the larger the cleavage energy and the smaller C the larger is the stress for the relaxed cleavage in comparison to the ideal brittle case.

Figure 6 shows the critical stresses vs. elastic modulus C. There is no obvious relation to be found, any simple direct relation will fail to give a reasonable estimation of the stress σ_b on the basis of the elastic properties. In fact, Eqs. A4 and A5 –as expressed by $\sigma_b/A \propto \sqrt{CG_b/A}$– relate the critical stress for ideal brittle cleavage to a combination of elastic properties (modulus C) and fracture properties (cleavage energy G_b). Therefore, according to our findings also quantities related to σ_b –such as Vicker's

hardness for brittle materials– cannot be reasonably estimated only on the basis of elastic properties.

IV. CONCLUSIONS

Cleavage decohesion with full relaxation of the atomic layers was described by a simple model which combines purely elastic response with abrupt breaking. Based on an UBER-like concept this model is is independent on the macroscopic thickness of the material. Although the cleavage energies G_r are smaller than their rigid counterparts G_b because of the surface relaxation, the critical stress σ_r is significantly larger (from 10% to 50%). The material when allowed to relax after the crack initialization needs larger crack sizes to break.

The crack size needed to break material l_r was determined from DFT data. We found obvious similarity of this parameter with L, the material parameter used for describing the localisation of the elastic energy for rigid cleavage. The agreement is truly remarkable, in particular for Al, rather ductile metal. In general some deviations of both parameters must be expected, because -in contrast to L which was derived within linear elastic limit- non-linear elastic effects are inherently involved in relaxed cleavage calculation. Very strong anharmonic effects can lead to a deviation from the ideal model, which was observed in the case of TiAl. Notably, the stacking of atomic planes seems to have no influence on the energy localisation, as emerges when one observes the parameters for [110] and [111] cleavage of NiAl.

The strong correlation of both parameters implies that -at the atomic scale- the local behaviour of the elastic energy in fracture of metals is a property of material. The results provide not only an insight into the elastic energy behaviour during brittle fracture but also lead to a simple estimate of the critical stress for the cohesive law derived from relaxed cleavage process.

APPENDIX A

Ideal brittle cleavage describes cleavage of a crystal in which the atoms in the cleaved blocks do not relax their positions after cleaving. For an analytic formulation of the ideal brittle cleavage process in loading mode I (as sketched in panel b of Fig. 1) we make use of the universal binding energy relation (UBER)[3] which proved to be a reliable model. When -in a given direction [hkl]- a single crystal is cleaved between two planes by an opening

x, the decohesion energy (or loss in bonding energy) is expressed by

$$E_b(x) = G_b \left[1 - \left(1 + \frac{x}{l_b} \right) \exp \left(-\frac{x}{l_b} \right) \right], \quad \text{(A1)}$$

The material and direction dependent parameters are the cleavage energy G_b and the critical length l_b at which the stress $\sigma_b(x) = dE_b/dx$ reaches its maximum,

$$\sigma_b = \frac{G_b}{e\, l_b}. \quad \text{(A2)}$$

It should be noted, that for a given direction $[hkl]$ the parameters G_b and l_b might also depend on the actual planes between which the material is cleaved. This happens for cases for which there are more than one geometrical possibility for cleavage (e.g. for the diamond lattice in $[111]$ direction with short and long interplanar distances).

As described in Ref. 2 cleavage and elasticity are assumed to be correlated at very small x for which we set equal the elastic energy and the Taylor series expansion of UBER up to x^2,

$$\frac{1}{2} \frac{G_b}{l_b^2} x^2 = \frac{1}{2} A L_b C \frac{x^2}{L_b^2} \quad \text{(A3)}$$

The elastic energy $E_e = CAL_b$ comprises the uniaxial elastic modulus C for a given direction $[hkl]$ and E_e is assumed to be localized in the volume $V = AL_b$. Now, a new materials parameter, the localization length L_b is introduced, which is independent of any macroscopic dimensions of the material. The elastic modulus C for a given direction $[hkl]$ is derived by the elastic constants,[35] which can be calculated by a DFT approach.

Using the relation of Eq. A3 the parameter l_b appearing in Eq. A2 can be eliminated, resulting in the definition of the critical stress per surface area,

$$\frac{\sigma_b}{A} = \frac{1}{e\sqrt{L_b}} \sqrt{C \frac{G_b}{A}}, \quad \text{(A4)}$$

In our recent study[2] we observed that for many materials L_b varies between 2 and 3 Å with an average value of $\overline{L_b} = 2.4$ Å . Inserting $\overline{L_b}$ into equation Eq. A4 the approximate relation[36]

$$\frac{\sigma_b}{A} \approx 0.75 \sqrt{C \frac{G_b}{A}}, \quad \text{(A5)}$$

In this equation, $\frac{\sigma_b}{A}$ is given in units of [GPa], and $\frac{G_b}{A}$ in units of [J/m^2]. In Eqs. A4,A5 the long-searched-for relation between cleavage (fracture) and elastic properties in terms of local quantities only has been established.

[1] A. A. Griffith, Phil. Trans. R. Soc. A **221**, 163 (1921).

[2] P. Lazar, R. Podloucky, and W. Wolf, Appl. Phys. Lett. **87**, 261910 (2005).

[3] J. H. Rose, J. R. Smith, and J. Ferrante, Phys. Rev. B **28**, 1835 (1983).

[4] A. Banerjea and J. R. Smith, Phys. Rev. B **37**, 6632 (1988).

[5] UBER fails for breaking strongly directed bonds, e.g. when cleaving diamond in the [111] direction between planes with the shortest layer-to-layer distance, because of maximum in the E_b curve at large x. This effect is due to re-ordering of strong covalent bonds. However, compared to other cleavage direction this particular [111] cleavage is highly unfavorable because of its very large stress and energy.

[6] P. E. Blöchl, Phys. Rev. B **50**, 17953 (1994).

[7] G. Kresse and D. Joubert, Phys. Rev. B **59**, 1758 (1999).

[8] J. P. Perdew and Y. Wang, Phys. Rev. B **45**, 13244 (1992).

[9] Y. Le Page and P. Saxe, Phys. Rev. B **63**, 174103 (2001).

[10] Y. Le Page and P. Saxe, Phys. Rev. B **65**, 104104 (2002).

[11] R. L. Hayes, M. Ortiz, and E. A. Carter, Phys. Rev. B **69**, 172104 (2004).

[12] O. Nguyen and M. Ortiz, J. Mech. Phys. Solids **50**, 1727 (2002).

[13] E. A. A. Jarvis, R. L. Hayes, and E. A. Carter, CHEMPHYSCHEM **2**, 55 (2001).

[14] B. Lawn, *Fracture of brittle solids* (Cambridge univ. press, New York, 1993).

[15] T. Hoshi, Y. Iguchi, and T. Fujiwara, Phys. Rev. B **72**, 075323 (2005).

[16] D. Hull, P. Beardmore, and A. P. Valentine, Philos. Mag. **12**, 1021 (1965).

[17] J. Riedle, P. Gumbsch, H. F. Fischmeister, V. G. Glebovski, and V. N. Semenov, Materials Letters **20**, 311 (1994).

[18] M. Ludwig and P. Gumbsch, Acta mater. **46**, 3135 (1998).

[19] J. H. Schneibel, J. A. Horton, and W. D. Porter, Mat. Sci. Eng. A **152**, 126 (1992).

[20] K. M. Chang, R. Darolia, and H. A. Lipsitt, Acta metall. mater. **40**, 2727 (1992).

[21] R. Darolia, K. M. Chang, and J. E. Hack, Intermetallics **1**, 65 (1993).

[22] J. M. Brzeski, J. E. H. R. Darolia, and R. Field, Mat. Sci. Eng. A **170**, 11 (1993).

[23] S. N. Sun, N. Kioussis, and M. Ciftan, Phys. Rev. B **54**, 3074 (1996).

[24] J. R. Rice, J. Mech. Phys. Solids **40**, 239 (1992).

[25] P. Lazar and R. Podloucky, Phys. Rev. B **73**, 104114 (2006).

[26] J. A. Hauch, D. Holland, M. P. Marder, and H. L. Swinney, Phys. Rev. Lett. **82**, 3823 (1999).

[27] A. M. Lomonosov and P. Hess, Phys. Rev. Lett. **89**, 095501 (2002).

[28] N. Bernstein and D. W. Hess, Phys. Rev. Lett. **91**, 025501 (2003).

[29] T. Cramer, A. Wanner, and P. Gumbsch, Phys. Rev. Lett. **85**, 788 (2000).

[30] A. Mattoni, L. Colombo, and F. Cleri, Phys. Rev. Lett. **95**, 115501 (2005).

[31] E. Orowan, Rep. Prog. Phys. **12**, 185 (1949).

[32] J. J. Gilman, in *The strength of ceramic crystals*, edited by C. Klingsberg (Gordon & Breach, New York, 1963), p. 240.

[33] S. Sidhu and C. S. Menon, J. Phys. Di: Appl. Phys. **34**, 465 (2001).

[34] In Griffith's paper[1] the surface energy $\gamma = \frac{1}{2}G$ being half of the cleavage energy was utilized. This relation is only valid only for high-symmetry cases for which both cleavage surfaces are equivalent.

[35] J. F. Nye, *Physical Properties of Crystals* (Oxford University Press, Oxford, 1993), e.g. for a cubic crystal the uniaxial rigid modulus C is defined in terms of the three cubic elastic constants c_{11}, c_{12}, c_{44} and the direction cosines h, k, l by $C = c_{11} - 2(c_{11} - c_{12} - 2c_{44})(h^2k^2 + h^2l^2 + k^2l^2)$.

[36] In Ref. 2 the prefactor was erronoulsy given as 0.24, because units of Å were used instead of nm. The correct factor is now $0.24\sqrt{10} = 0.75$.